EUROPEAN ORGANIZATION FOR NUCLEAR RESEARCH

CERN-EP-2001-040
17 May 2001

Search for Single Leptoquark and Squark Production in Electron-Photon Scattering at $\sqrt{s_{\mathrm{ee}}} = 189$ GeV at LEP

The OPAL Collaboration

Abstract

A search for first generation scalar and vector leptoquarks (LQ) as well as for squarks ($\tilde{\mathrm{q}}$) in R-parity violating SUSY models has been performed using $\mathrm{e^+e^-}$ collisions collected with the OPAL detector at LEP at an $\mathrm{e^+e^-}$ centre-of-mass energy $\sqrt{s_{\mathrm{ee}}}$ of 189 GeV. The data correspond to an integrated luminosity of about 160 pb^{-1}. The dominant process for this search is $\mathrm{eq} \to \mathrm{LQ}/\tilde{\mathrm{q}} \to \mathrm{eq}, \nu\mathrm{q}$, where a photon, which has been radiated by one of the beam electrons, serves as a source of quarks. The numbers of selected events found in the two decay channels are in agreement with the expectations from Standard Model processes. This result allows to set lower limits at the 95 % confidence level on the mass of first generation scalar and vector leptoquarks, and of squarks in R-parity violating SUSY models. For Yukawa couplings λ to fermions larger than $\sqrt{4\pi\alpha_{\mathrm{em}}}$, the mass limits range from 121 GeV/c^2 to 175 GeV/c^2 (149 GeV/c^2 to 188 GeV/c^2) depending on the branching ratio β of the scalar (vector) leptoquark state. Furthermore, limits are set on the Yukawa couplings λ for leptoquarks and λ'_{1jk} for squarks, and on β as a function of the scalar leptoquark/squark mass.

(To be submitted to Eur. Phys. J. C)

The OPAL Collaboration

G. Abbiendi[2], C. Ainsley[5], P.F. Åkesson[3], G. Alexander[22], J. Allison[16], G. Anagnostou[1], K.J. Anderson[9], S. Arcelli[17], S. Asai[23], D. Axen[27], G. Azuelos[18,a], I. Bailey[26], A.H. Ball[8], E. Barberio[8], R.J. Barlow[16], R.J. Batley[5], T. Behnke[25], K.W. Bell[20], G. Bella[22], A. Bellerive[9], S. Bethke[32], O. Biebel[32], I.J. Bloodworth[1], O. Boeriu[10], P. Bock[11], J. Böhme[25], D. Bonacorsi[2], M. Boutemeur[31], S. Braibant[8], L. Brigliadori[2], R.M. Brown[20], H.J. Burckhart[8], J. Cammin[3], R.K. Carnegie[6], B. Caron[28], A.A. Carter[13], J.R. Carter[5], C.Y. Chang[17], D.G. Charlton[1,b], P.E.L. Clarke[15], E. Clay[15], I. Cohen[22], J. Couchman[15], A. Csilling[15,i], M. Cuffiani[2], S. Dado[21], G.M. Dallavalle[2], S. Dallison[16], A. De Roeck[8], E.A. De Wolf[8], P. Dervan[15], K. Desch[25], B. Dienes[30], M.S. Dixit[6,a], M. Donkers[6], J. Dubbert[31], E. Duchovni[24], G. Duckeck[31], I.P. Duerdoth[16], E. Etzion[22], F. Fabbri[2], L. Feld[10], P. Ferrari[12], F. Fiedler[8], I. Fleck[10], M. Ford[5], A. Frey[8], A. Fürtjes[8], D.I. Futyan[16], P. Gagnon[12], J.W. Gary[4], G. Gaycken[25], C. Geich-Gimbel[3], G. Giacomelli[2], P. Giacomelli[2], D. Glenzinski[9], J. Goldberg[21], C. Grandi[2], K. Graham[26], E. Gross[24], J. Grunhaus[22], M. Gruwé[08], P.O. Günther[3], A. Gupta[9], C. Hajdu[29], G.G. Hanson[12], K. Harder[25], A. Harel[21], M. Harin-Dirac[4], M. Hauschild[8], C.M. Hawkes[1], R. Hawkings[8], R.J. Hemingway[6], C. Hensel[25], G. Herten[10], R.D. Heuer[25], J.C. Hill[5], K. Hoffman[8], R.J. Homer[1], D. Horváth[29,c], K.R. Hossain[28], R. Howard[27], P. Hüntemeyer[25], P. Igo-Kemenes[11], K. Ishii[23], A. Jawahery[17], H. Jeremie[18], C.R. Jones[5], P. Jovanovic[1], T.R. Junk[6], N. Kanaya[23], J. Kanzaki[23], G. Karapetian[18], D. Karlen[6], V. Kartvelishvili[16], K. Kawagoe[23], T. Kawamoto[23], R.K. Keeler[26], R.G. Kellogg[17], B.W. Kennedy[20], D.H. Kim[19], K. Klein[11], A. Klier[24], S. Kluth[32], T. Kobayashi[23], M. Kobel[3], T.P. Kokott[3], S. Komamiya[23], R.V. Kowalewski[26], T. Krämer[25], T. Kress[4], P. Krieger[6], J. von Krogh[11], D. Krop[12], T. Kuhl[3], M. Kupper[24], P. Kyberd[13], G.D. Lafferty[16], H. Landsman[21], D. Lanske[14], I. Lawson[26], J.G. Layter[4], A. Leins[31], D. Lellouch[24], J. Letts[12], L. Levinson[24], R. Liebisch[11], J. Lillich[10], C. Littlewood[5], A.W. Lloyd[1], S.L. Lloyd[13], F.K. Loebinger[16], G.D. Long[26], M.J. Losty[6,a], J. Lu[27], J. Ludwig[10], A. Macchiolo[18], A. Macpherson[28,l], W. Mader[3], S. Marcellini[2], T.E. Marchant[16], A.J. Martin[13], J.P. Martin[18], G. Martinez[17], T. Mashimo[23], P. Mättig[24], W.J. McDonald[28], J. McKenna[27], T.J. McMahon[1], R.A. McPherson[26], F. Meijers[8], P. Mendez-Lorenzo[31], W. Menges[25], F.S. Merritt[9], H. Mes[6,a], A. Michelini[2], S. Mihara[23], G. Mikenberg[24], D.J. Miller[15], S. Moed[21], W. Mohr[10], A. Montanari[2], T. Mori[23], K. Nagai[13], I. Nakamura[23], H.A. Neal[33], R. Nisius[8], S.W. O'Neale[1], F.G. Oakham[6,a], F. Odorici[2], A. Oh[8], A. Okpara[11], M.J. Oreglia[9], S. Orito[23], C. Pahl[32], G. Pásztor[8,i], J.R. Pater[16], G.N. Patrick[20], J.E. Pilcher[9], J. Pinfold[28], D.E. Plane[8], B. Poli[2], J. Polok[8], O. Pooth[8], A. Quadt[8], K. Rabbertz[8], C. Rembser[8], P. Renkel[24], H. Rick[4], N. Rodning[28], J.M. Roney[26], S. Rosati[3],

K. Roscoe[16], Y. Rozen[21], K. Runge[10], D.R. Rust[12], K. Sachs[6], T. Saeki[23], O. Sahr[31], E.K.G. Sarkisyan[8,m], C. Sbarra[26], A.D. Schaile[31], O. Schaile[31], P. Scharff-Hansen[8], M. Schröder[8], M. Schumacher[25], C. Schwick[8], W.G. Scott[20], R. Seuster[14,g], T.G. Shears[8,j], B.C. Shen[4], C.H. Shepherd-Themistocleous[5], P. Sherwood[15], A. Skuja[17], A.M. Smith[8], G.A. Snow[17], R. Sobie[26], S. Söldner-Rembold[10,e], S. Spagnolo[20], F. Spano[9], M. Sproston[20], A. Stahl[3], K. Stephens[16], K. Stoll[10], D. Strom[19], R. Ströhmer[31], L. Stumpf[26], B. Surrow[8], S.D. Talbot[1], S. Tarem[21], M. Tasevsky[8], R.J. Taylor[15], R. Teuscher[9], J. Thomas[15], M.A. Thomson[5], E. Torrence[9], D. Toya[23], T. Trefzger[31], I. Trigger[8], Z. Trócsányi[30,f], E. Tsur[22], M.F. Turner-Watson[1], I. Ueda[23], B. Ujvári[30,f], B. Vachon[26], C.F. Vollmer[31], P. Vannerem[10], M. Verzocchi[8], H. Voss[8], J. Vossebeld[8], D. Waller[6], C.P. Ward[5], D.R. Ward[5], P.M. Watkins[1], A.T. Watson[1], N.K. Watson[1], P.S. Wells[8], T. Wengler[8], N. Wermes[3], D. Wetterling[11] G.W. Wilson[16], J.A. Wilson[1], T.R. Wyatt[16], S. Yamashita[23], V. Zacek[18], D. Zer-Zion[8,k]

[1]School of Physics and Astronomy, University of Birmingham, Birmingham B15 2TT, UK
[2]Dipartimento di Fisica dell' Università di Bologna and INFN, I-40126 Bologna, Italy
[3]Physikalisches Institut, Universität Bonn, D-53115 Bonn, Germany
[4]Department of Physics, University of California, Riverside CA 92521, USA
[5]Cavendish Laboratory, Cambridge CB3 0HE, UK
[6]Ottawa-Carleton Institute for Physics, Department of Physics, Carleton University, Ottawa, Ontario K1S 5B6, Canada
[7]Centre for Research in Particle Physics, Carleton University, Ottawa, Ontario K1S 5B6, Canada
[8]CERN, European Organisation for Nuclear Research, CH-1211 Geneva 23, Switzerland
[9]Enrico Fermi Institute and Department of Physics, University of Chicago, Chicago IL 60637, USA
[10]Fakultät für Physik, Albert-Ludwigs-Universität, D-79104 Freiburg, Germany
[11]Physikalisches Institut, Universität Heidelberg, D-69120 Heidelberg, Germany
[12]Indiana University, Department of Physics, Swain Hall West 117, Bloomington IN 47405, USA
[13]Queen Mary and Westfield College, University of London, London E1 4NS, UK
[14]Technische Hochschule Aachen, III Physikalisches Institut, Sommerfeldstrasse 26-28, D-52056 Aachen, Germany
[15]University College London, London WC1E 6BT, UK
[16]Department of Physics, Schuster Laboratory, The University, Manchester M13 9PL, UK

[17]Department of Physics, University of Maryland, College Park, MD 20742, USA
[18]Laboratoire de Physique Nucléaire, Université de Montréal, Montréal, Quebec H3C 3J7, Canada
[19]University of Oregon, Department of Physics, Eugene OR 97403, USA
[20]CLRC Rutherford Appleton Laboratory, Chilton, Didcot, Oxfordshire OX11 0QX, UK
[21]Department of Physics, Technion-Israel Institute of Technology, Haifa 32000, Israel
[22]Department of Physics and Astronomy, Tel Aviv University, Tel Aviv 69978, Israel
[23]International Centre for Elementary Particle Physics and Department of Physics, University of Tokyo, Tokyo 113-0033, and Kobe University, Kobe 657-8501, Japan
[24]Particle Physics Department, Weizmann Institute of Science, Rehovot 76100, Israel
[25]Universität Hamburg/DESY, II Institut für Experimental Physik, Notkestrasse 85, D-22607 Hamburg, Germany
[26]University of Victoria, Department of Physics, P O Box 3055, Victoria BC V8W 3P6, Canada
[27]University of British Columbia, Department of Physics, Vancouver BC V6T 1Z1, Canada
[28]University of Alberta, Department of Physics, Edmonton AB T6G 2J1, Canada
[29]Research Institute for Particle and Nuclear Physics, H-1525 Budapest, P O Box 49, Hungary
[30]Institute of Nuclear Research, H-4001 Debrecen, P O Box 51, Hungary
[31]Ludwigs-Maximilians-Universität München, Sektion Physik, Am Coulombwall 1, D-85748 Garching, Germany
[32]Max-Planck-Institute für Physik, Föhring Ring 6, 80805 München, Germany
[33]Yale University,Department of Physics,New Haven, CT 06520, USA

[a] and at TRIUMF, Vancouver, Canada V6T 2A3
[b] and Royal Society University Research Fellow
[c] and Institute of Nuclear Research, Debrecen, Hungary
[e] and Heisenberg Fellow
[f] and Department of Experimental Physics, Lajos Kossuth University, Debrecen, Hungary
[g] and MPI München
[i] and Research Institute for Particle and Nuclear Physics, Budapest, Hungary
[j] now at University of Liverpool, Dept of Physics, Liverpool L69 3BX, UK
[k] and University of California, Riverside, High Energy Physics Group, CA 92521, USA
[l] and CERN, EP Div, 1211 Geneva 23
[m] and Tel Aviv University, School of Physics and Astronomy, Tel Aviv 69978, Israel.

1 Introduction

Leptoquarks (LQ) are coloured spin 0 or spin 1 particles carrying both baryon (B) and lepton (L) quantum numbers. They appear in many extensions of the Standard Model as a consequence of the symmetry between the lepton and quark sectors. The Buchmüller-Rückl-Wyler (BRW) model [1] used in this paper assumes lepton and baryon number conservation. Moreover the simplifying assumption is made that a given leptoquark couples to just one family of fermions which means that only first generation leptoquarks can be produced in electron-photon scattering. The first generation leptoquarks may decay into either an electron[1] and a quark or into a neutrino and a quark. The branching ratio of the decay into an electron and a quark is commonly denoted by β. Table 1 shows all the possible leptoquark states considered in this paper (scalar and vector) using the most common nomenclature [2] along with their electric charge and fermion number $F = L + 3B$. The branching ratios β given in this table assume that the leptoquarks couple only to Standard Model particles. To respect the existing limits on the product $\lambda_{\mathrm{L}} \cdot \lambda_{\mathrm{R}}$ we assume that for the scalar states S_0 and $\mathrm{S}_{1/2}$ and the vector states V_0 and $\mathrm{V}_{1/2}$ either the left-handed or the right-handed coupling must vanish, i.e. $\lambda_{\mathrm{L}} \cdot \lambda_{\mathrm{R}} = 0$.

At an $\mathrm{e^+e^-}$ collider different diagrams are expected to contribute to single leptoquark production in electron-photon collisions [4, 5, 6, 7, 8]. The dominant diagram is eq $\rightarrow$ LQ (Fig. 1), where a photon, which has been radiated by one of the beam electrons, serves as a source of quarks through its fluctuations into hadronic states. The electron-quark interaction produces a leptoquark which is assumed to decay subsequently into an electron or a neutrino, and a quark. The photon remnant may disappear down the beam-pipe or add some activity in the forward region of the detector. The diagrams shown in Fig. 2 are also relevant, whereas $\mathrm{e^+e^-}$ annihilation diagrams with a single leptoquark radiated in the final state and diagrams with quark and/or leptoquark exchange in the t-channel but without photon exchange are suppressed. The signature of single leptoquark events is one hadronic jet with high transverse momentum, balanced either by one isolated electron or by missing transverse energy due to the neutrino. Both topologies are studied in this paper.

Squarks ($\tilde{\mathrm{q}}$) in supersymmetric models with R-parity violation have the same production mechanism as some leptoquarks. R-parity is a quantum number which equals $+1$ for particles and -1 for their superpartners. Table 1 shows the correspondence between the squark and the leptoquark states. R-parity conserving decays are possible for squarks, in addition to the R-parity violating leptoquark

[1] Charge conjugation is implied throughout this paper for all particles, e.g. positrons are also referred to as electrons.

decay modes. The ratio between the R-parity conserving and violating modes depends on the parameters of supersymmetry and on the size of the coupling. For this analysis the branching ratio for R-parity conserving decays has been set to zero and consequently β has the same value for squarks and the corresponding leptoquarks. Supersymmetry allows only left-handed couplings to leptons for these states. In the most general superpotential of the Minimal Supersymmetric Model (MSSM), the renormalizable gauge invariant operator which describes the coupling of squarks to quarks and leptons and violates R-parity is $\lambda'_{ijk} L^i_{\rm L} Q^j_{\rm L} \bar{D}^k_{\rm R}$ [3], where i, j and k are generation indices of the left-handed doublet superfields of leptons ($L_{\rm L}$) and quarks ($Q_{\rm L}$), and right-handed singlets of down-type quarks ($\bar{D}_{\rm R}$). Only couplings λ'_{1jk} to first generation leptons are considered in this paper.

Several experiments have searched for leptoquarks. DELPHI analysed the single scalar and vector leptoquark production setting limits on the mass ranging from 134 GeV/c^2 to 171 GeV/c^2 at an e^+e^- centre-of-mass energy $\sqrt{s}_{\rm ee}$ of 183 GeV [9] and for a Yukawa coupling $\lambda > \sqrt{4\pi\alpha_{\rm em}}$. The H1 collaboration at HERA has searched for leptoquarks in deep-inelastic neutral current (NC) and charged current (CC) electron-proton scattering at high Q^2 [10]. First generation scalar (vector) leptoquarks have been excluded for masses up to 275 GeV/c^2 (284 GeV/c^2) for $\lambda > \sqrt{4\pi\alpha_{\rm em}}$ and fermion number $F = 0$, while masses up to about 200 GeV/c^2 have been excluded for $|F| = 2$ leptoquarks. Leptoquark limits as a function of the assumed couplings have also been obtained from fermion pair production at LEP2 at $\sqrt{s}_{\rm ee} = 130 - 183$ GeV [11].

Leptoquark pair production limits have been obtained by the LEP experiments at $\sqrt{s}_{\rm ee} = M_{\rm Z}$ [12] and at $\sqrt{s}_{\rm ee} = 183$ GeV [13], and by the D0 [14] and CDF experiments [15] for leptoquarks of the three generations. The leptoquark pair production limits are independent of the Yukawa coupling λ in $\overline{\rm p}$p scattering. In e^+e^- scattering the leptoquark pair production cross-section can be considered independent of λ only in the region of small λ where t-channel quark exchange can be neglected compared to the s-channel diagram. At LEP2 energies, $\sqrt{s}_{\rm ee} = 183$ GeV, the mass limits for first generation leptoquarks vary between 80 GeV/c^2 and 90 GeV/c^2, depending on the leptoquark state [13]. Scalar leptoquarks of charge $-1/3$ are only excluded for $M_{\rm LQ} < M_{\rm Z}/2$ [12]. A combination of the CDF and D0 search results for a first generation scalar leptoquark yields a lower mass limit of 242 GeV/c^2 for $\beta = 1$ [16]. The CDF and D0 collaborations [17] as well as the four LEP experiments [18] have also searched for pair production of R-parity violating squarks.

Leptoquark pair production limits obtained at LEP are sensitive to the mass region $M_{\rm LQ} < \sqrt{s_{\rm ee}}/2$, whereas single leptoquarks can be produced almost up to the kinematic limit, $M_{\rm LQ} = \sqrt{s_{\rm ee}}$. Even though the leptoquark mass range covered by CDF and D0 in $\bar{\rm p}$p scattering is higher for most leptoquark states, the

scalar LQ($\tilde{q}$)	charge	F	decay mode	β
$\tilde{S}_0$ (or $\tilde{d}_R$)	-1/3	2	$e_L^- u$, $\nu_L d$	1/2
			$e_R^- u$	1
S_0	-4/3	2	$e_R^- d$	1
$\tilde{S}_{1/2}$ (or $\tilde{\bar{d}}_L$)	+1/3	0	$\nu_L \bar{d}$	0
$\tilde{S}_{1/2}$ (or $\tilde{\bar{u}}_L$)	-2/3	0	$e_L^- \bar{d}$	1
S_1	+2/3	2	$\nu_L u$	0
	-1/3		$\nu_L d$, $e_L^- u$	1/2
	-4/3		$e_L^- d$	1
$S_{1/2}$	-2/3	0	$\nu_L \bar{u}$	0
			$e_R^- \bar{d}$	1
	-5/3		$e_L^- \bar{u}$ or $e_R^- \bar{u}$	1
vector LQ	charge	F	decay mode	β
$V_{1/2}$	-1/3	2	$\nu_L d$	0
			$e_R^- u$	1
	-4/3		$e_R^- d$ or $e_L^- d$	1
$\tilde{V}_{1/2}$	+2/3	2	$\nu_L u$	0
	-1/3		$e_L^- u$	1
V_0	-2/3	0	$e_L^- \bar{d}$, $\nu_L \bar{u}$	1/2
			$e_R^- \bar{d}$	1
V_1	+1/3	0	$\nu_L \bar{d}$	0
	-2/3		$e_L^- \bar{d}$, $\nu_L \bar{u}$	1/2
	-5/3		$e_L^- \bar{u}$	1
$\tilde{V}_0$	-5/3	0	$e_R^- \bar{u}$	1

Table 1: All possible scalar (S) leptoquarks/squarks and vector (V) leptoquarks in the BRW model with their electric charge in units of e, their fermion number F, their decay modes and the corresponding branching ratio β for the decay into an electron and a quark.

analysis presented here is more sensitive in the low β region ($\beta \to 0$). For $\beta \equiv 0$ no production in eq collisions is possible. In addition, this search is also sensitive to the production of ec (and es) states, but only flavour-diagonal couplings λ are considered in this paper.

We present a search for leptoquarks with $M_{\mathrm{LQ}} > 80$ GeV in electron-photon scattering using data corresponding to an integrated luminosity of 164.7 pb^{-1} (eq channel) and 158.4 pb^{-1} (νq channel) at $\mathrm{e^+e^-}$ centre-of-mass energies of 189 GeV.

2 The OPAL detector

The OPAL detector is described in detail in [19]. It is a multipurpose apparatus having nearly complete solid angle coverage with excellent hermeticity. The central detector consists of two layers of silicon micro-strip detectors [20] surrounding the beam-pipe and a system of gaseous tracking chambers inside a 0.435 T solenoidal magnetic field.

The lead-glass electromagnetic calorimeter (ECAL) with a presampler is located outside the magnet coil. It provides, in combination with the forward calorimeters (FD), the forward scintillating tile counter (the "MIP plug") [21], and the silicon-tungsten luminometer (SW) [22], a geometrical acceptance down to 25 mrad from the beam direction. The SW luminometer measures the integrated luminosity using small-angle Bhabha scattering events [23]. The magnet return yoke is instrumented for hadron calorimetry (HCAL). It is surrounded by several layers of muon chambers.

3 Kinematics and Monte Carlo simulations

The Monte Carlo simulation of the process $\mathrm{e^+e^-} \to \mathrm{LQ} + \mathrm{X}$ is done with the program ERATO-LQ [25] which can generate all the states listed in Table 1 and calculates the cross-sections for the scalar and vector states[2].

The total cross-section for the production of leptoquarks of mass M_{LQ} can be written as a convolution of the probability to find a photon with the momentum fraction z in the electron, approximated here by the Weizsäcker-Williams effective photon distribution $f_{\gamma/e}(z)$ [24], and the probability to find a quark in the

[2] All total cross-sections in this paper are defined as a sum of the particle and the anti-particle state.

photon. This probability can be parametrised by parton distribution functions (pdf) $f_{\mathrm{q}/\gamma}(x,\mu^2)$ of the photon, which are evaluated at the scale $\mu^2 = M^2$ [4]. The Bjorken scaling variable x is given by $x = M^2/zs$. With these assumptions the total cross-section for scalar leptoquark production is:

$$\sigma(\mathrm{e^+e^-} \to \mathrm{LQ} + \mathrm{X}) = \frac{\lambda^2\pi}{2s}\int_{M^2/s}^{1}\frac{dz}{z} f_{\gamma/e}(z) f_{\mathrm{q}/\gamma}(M^2/(zs), M^2) \qquad (1)$$

where $f_{\mathrm{q}/\gamma}(M^2/(zs), M^2)$ is obtained by convoluting the parton level cross section with the quark distribution $f_{\mathrm{q}/\gamma}(z, M^2)$ in the photon. In case of unpolarised electron beams, the total cross-section for the production of vector leptoquarks is twice as large as the cross-section for scalar leptoquarks [1]. This approach based on the pdf is used in the calculations of the diagram shown in Fig. 1 by Donchesky [4] and it is also implemented in the Monte Carlo generator PYTHIA [26].

However, PYTHIA can only generate scalar leptoquarks with charge $-1/3$. It has therefore only been used to check the cross-sections calculated by ERATO-LQ [25]. This Monte Carlo generator uses a perturbative calculation of the diagrams in Fig. 1 and 2. It is expected to give the correct angular distributions both for the scalar and vector leptoquarks.

Cross-sections calculated with ERATO-LQ and PYTHIA using $\lambda = \sqrt{4\pi\alpha_{\mathrm{em}}}$ and charge $-1/3$ (e.g for S_0) are shown in Table 2. Using a different parametrisation of the pdf, GRV [27] instead of SaS-1D [28], has almost no effect on the resulting cross-section. In ERATO-LQ the exact total cross-section given in [6], taking into account all possible diagrams, can also be calculated. In comparison, the total cross-section calculated perturbatively by the MC generator ERATO-LQ is $10-20\%$ smaller than the exact total cross-section used to calculate the limits.

ERATO-LQ generates the four-vectors of the direct decay products of the leptoquark. A scalar leptoquark decays isotropically in its rest frame leading to a flat distribution in the variable $y = (1+\cos\theta^*)$, where θ^* is the decay angle of the lepton relative to the incident quark in the leptoquark centre-of-mass frame. The decay angles in the decays of vector leptoquarks are distributed according to $\mathrm{d}\sigma/\mathrm{d}y \propto (1-y)^2$. The simulated photon is always real, i.e., the negative squared four-momentum of the photon, Q^2, is identical to zero.

The partial decay widths of a scalar (S) and a vector (V) leptoquark are

$$\Gamma_{\mathrm{S}} = \frac{3}{2}\Gamma_{\mathrm{V}} = \frac{\lambda^2}{16\pi}M_{\mathrm{LQ}}. \qquad (2)$$

Since the leptoquark carries colour, it could hadronise before its decay into fermions. This effect is taken into account in the systematic uncertainties but not

	M_{LQ} [GeV/c^2]	80	100	120	140	160	170	180
PYTHIA (GRV)	σ_{tot} [pb]	2.78	1.31	0.64	0.32	0.14	0.083	0.046
PYTHIA (SaS-1D)	σ_{tot} [pb]	2.77	1.30	0.64	0.32	0.14	0.086	0.046
ERATO-LQ [6] (exact)	σ_{tot} [pb]	2.81	1.46	0.77	0.40	0.18	0.102	0.037
ERATO-LQ (perturb.)	σ_{tot} [pb]	2.32	1.21	0.65	0.34	0.16	0.085	0.031

Table 2: The total cross-section for the single production of the state S_0 with charge $-1/3$ as a function of the leptoquark mass M_{LQ} calculated by the Monte Carlo generators ERATO-LQ and PYTHIA at $\sqrt{s}_{\mathrm{ee}} = 189$ GeV using $\lambda = \sqrt{4\pi\alpha_{\mathrm{em}}}$.

in the standard Monte Carlo simulation, since it should only be important for $\Gamma_{\mathrm{S,V}} \ll \Lambda_{\mathrm{QCD}}$. The decay width Γ_{S} is 16 MeV for $\lambda = 0.1$ and $M_{\mathrm{LQ}} = 80$ GeV/c^2.

JETSET [26] is used to perform the hadronisation of the leptoquark decay products. It has been checked with ERATO-LQ that the event properties of the different leptoquark states are very similar which allows to simplify the generation considerably: For each of the seven masses listed in Table 2, samples of 3000 events for scalar and vector leptoquarks were generated for the two leptoquark decay modes separately and only for one state. Also, no extra squark events needed to be generated.

All relevant Standard Model background processes have been studied using Monte Carlo generators. Multi-hadronic events ($\mathrm{e^+e^-} \to \mathrm{q\overline{q}}(\gamma)$) have been simulated with PYTHIA 5.722 [26]. KORALZ 4.02 [29] has been used to generate the process $\mathrm{e^+e^-} \to \tau^+\tau^-$ and BHWIDE [30] to generate the Bhabha process $\mathrm{e^+e^-} \to \mathrm{e^+e^-}$.

Deep inelastic eγ events in the range $Q^2 > 4.5$ GeV^2 including charged current deep inelastic scattering (CC DIS) events have been simulated with HERWIG 5.8 [31]. PHOJET 1.10 [32] has been used to generate hadronic two-photon events (i.e. $\mathrm{e^+e^-} \to \mathrm{e^+e^-}$ hadrons) in the range $Q^2 < 4.5$ GeV^2. Leptonic two-photon events have been generated with Vermaseren [33]. The events generated with HERWIG, PHOJET and Vermaseren are called two-photon events. An alternative hadronic two-photon sample for systematic studies has been generated using F2GEN [34] for $Q^2 > 4.5$ GeV^2 and PYTHIA for $Q^2 < 4.5$ GeV^2. Other processes with four fermions in the final states, including W pair production, have been simulated with grc4f [35] and an alternative sample has been generated with KORALW [36]. The generated signal events and all the background Monte

Carlo events have been passed through a full detector simulation and the same reconstruction algorithms as the real data.

4 Event analysis

We search for events with one hadronic jet and either an electron or missing energy balancing the transverse momentum of this jet. The analysis uses tracks measured in the central tracking devices, clusters measured in the ECAL, the HCAL, the FD and the SW. In addition to quality requirements which ensure that the tracks have their origin close to the e^+e^- interaction point, tracks must have more than 20 hits in the central jet chamber and more than half the number of hits expected for the given track. The transverse momentum of the track with respect to the beam direction must be greater than 120 MeV. Tracks with a momentum error larger than the momentum itself are rejected if they have fewer than 80 hits. Calorimeter clusters have to pass energy threshold cuts to suppress noise. To avoid double counting of particle momenta, a matching algorithm between tracks and clusters is applied [37]. Clusters are rejected if the energy of the cluster is less than expected from the momentum of an associated track. If the cluster energy exceeds the expected energy by more than what is expected from the resolution, the expected energy is subtracted from the cluster energy. In this case the track momentum and the reduced energy of the cluster are counted separately.

The tracks and remaining clusters are used as input to the jet finding algorithm and to determine the missing transverse energy of the event. Jets are reconstructed using a cone jet finding algorithm with a cone size $R = 1$ and a minimum transverse jet energy E_{T} of 15 GeV [37]. The cone size R is defined as $R = \sqrt{(\Delta\eta)^2 + (\Delta\phi)^2}$, with $\eta = -\ln\tan(\theta/2)$ being the pseudorapidity, ϕ the azimuthal angle and θ the polar angle in the laboratory frame in radians. $\Delta\eta$ and $\Delta\phi$ are the differences between the cone axis and the particle direction. No cut on the pseudorapidity of the jet is used at this stage.

4.1 The electron plus hadronic jet channel

In this search the selection cuts were optimised for a leptoquark decaying into a single quark and an isolated electron. The electron is identified by requiring a minimum of 20 hits used in the measurement of the specific energy loss, $\mathrm{d}E/\mathrm{d}x$, and a $\mathrm{d}E/\mathrm{d}x$ probability for the electron hypothesis of more than 1%. Furthermore, the ratio of the total energy of the electron measured in the ECAL to

the momentum of the track associated to this ECAL cluster must lie between 0.7 and 2. The identified electron with the largest momentum was assumed to be the electron from the leptoquark decay. Since the electron is included in the jet search, it is usually reconstructed as a jet. Candidate leptoquark events are selected based on the following cuts, which are identical for scalar and vector leptoquarks:

- The event must contain more than four tracks ($n_{\mathrm{ch}} > 4$).
- Exactly two jets must have been reconstructed ($n_{\mathrm{jet}} = 2$). One of the jets must contain the highest energy electron.
- The highest energy electron must have an energy E_{e} greater than 2 GeV. The electron energy E_{e} is the energy of the calorimeter clusters matched to the electron track. This cut is effective against all sources of Standard Model background, especially two-photon events.
- The jet not containing the electron must consist of more than six particles ($n_{\mathrm{qj}} > 6$), where the number n_{qj} of particles is defined as the sum of the number of tracks and calorimeter clusters after matching. This cut reduces the number of $\mathrm{e^+e^-} \to \tau^+\tau^-$ and the number of Bhabha events and also some of the remaining leptonic two-photon events.
- The total energy E_{HCAL} measured in the hadronic calorimeter has to be greater than 1 GeV. This cut is effective against Bhabha events.

After this preselection, 5739 data events remain. The selection efficiencies are given in Table 3. They are significantly smaller for the vector leptoquark states than for the scalar leptoquark states due to the angular distribution of the decay electrons which is peaked at $\cos\theta = \pm 1$ for vector leptoquark states. The following set of cuts is applied to the remaining events:

EQ1) To ensure that most of the measured energy comes from the two jets, the energy E_{qj} of the hadronic jet and the electron energy E_{e} must add up to more than 80% of the visible energy E_{vis}, i.e. $((E_{\mathrm{qj}} + E_{\mathrm{e}})/E_{\mathrm{vis}} > 0.8)$. This cut is efficient against multihadronic and four-fermion events (Fig. 3a).

EQ2) The ratio of the missing transverse energy $\not\!\!E_{\mathrm{T}}$ and the invariant mass M_{jj} of the two jets has to be $\not\!\!E_{\mathrm{T}}/M_{\mathrm{jj}} < 0.15$. The invariant mass M_{jj} of the two jets is calculated from the four-vectors of the two reconstructed jets. This cut reduces the four-fermion background by a factor two (Fig. 3b).

EQ3) Since the electron is expected to be isolated, the difference between the electron energy E_e and the energy E_{ej} of the jet which contains the electron has to be smaller than 2 GeV ($|E_e - E_{ej}| < 2$ GeV). This eliminates most of the remaining $e^+e^- \to q\overline{q}(\gamma)$ events (Fig. 3c).

EQ4) The electron must lie in the angular region defined by $|\cos\theta_e| < 0.8$ (Fig. 3d). This cut rejects mainly two-photon events with a scattered electron within the detector acceptance.

In Table 3 the number of data events and the expected number of Standard Model background events taken from the Monte Carlo are shown after the preselection and after each subsequent cut. The number of Monte Carlo events has been normalised to the data luminosity. The selection efficiencies for three different scalar and vector leptoquark masses are also given.

cuts		Pre-	$\frac{E_{qj}+E_e}{E_{vis}}$	$\not\!\!E_T/M_{jj}$	$\lvert E_e - E_{ej}\rvert$	$\lvert\cos\theta_e\rvert$
M_{LQ} [GeV/c^2]	state	selection	(EQ1)	(EQ2)	(EQ3)	(EQ4)
80	scalar	49.6%	44.7%	39.4%	37.9%	28.4%
120		61.4%	58.7%	54.1%	51.6%	45.1%
160		70.7%	70.5%	65.4%	60.2%	55.0%
80	vector	37.0%	31.2%	27.8%	26.7%	12.3%
120		50.4%	47.5%	43.9%	41.6%	29.4%
160		61.5%	61.3%	57.4%	54.0%	44.2%
$e^+e^- \to q\overline{q}$		4834	200.1	160.1	2.7	2.2 ± 0.2
$e^+e^- \to \tau^+\tau^-$		13.1	5.2	2.7	0.7	0.5 ± 0.1
$e^+e^- \to e^+e^-$		0.5	0.5	0.5	0.5	0.2 ± 0.1
$e^+e^- \to 4$ fermions		817.2	72.8	33.0	18.2	12.8 ± 0.5
two-photon		62.2	30.0	26.2	25.5	6.3 ± 1.0
total BG		5727	308.5	222.4	47.5	21.9 ± 1.1
data		5739	270	194	36	21

Table 3: Selection efficiencies for three different leptoquark masses for scalar and vector leptoquarks. The remaining number of data events and the expected number of background (BG) events are also listed after each cut of the electron plus hadronic jet selection. The Monte Carlo background is normalised to the data luminosity of 164.7 pb^{-1} at 189 GeV. The errors on the Monte Carlo background are statistical.

Figs. 3a-d show the distributions of some of the cut variables for data, Standard Model background and the leptoquark state $\tilde{V}_0$ with a mass of 120 GeV.

The data distributions are in general well described by the Monte Carlo simulation. After all cuts the Standard Model background is expected to be mainly due to four-fermion and two-photon interactions.

The $|\cos\theta_e|$ distribution depends strongly on the leptoquark mass. This is shown in Fig. 3d where an additional distribution for a leptoquark mass of 80 GeV has been added. The cut $|\cos\theta_e| < 0.8$ is necessary to reduce the background from two-photon events, but it also significantly reduces the efficiency for small M_{LQ}.

Fig. 4a shows the selection efficiencies after all cuts as determined with ERATO-LQ as a function of the generated leptoquark mass M_{LQ}. Fig. 4b shows the distributions of M_{jj} for data, Standard Model background and for the state $\tilde{V}_0$ using $\lambda = \sqrt{4\pi\alpha_{em}}$ with $M_{LQ} = 80$ GeV/c^2 and 120 GeV/c^2. After all cuts, 21 events remain in the data which is in good agreement with the predicted 21.9 ± 1.1 (stat) Standard Model background events.

4.2 The neutrino plus hadronic jet channel

In the case of the decay of a leptoquark into a neutrino and a single quark, the search has to be optimised for a single hadronic jet in the detector. Its transverse energy $E_{T,jet}$ must be balanced by the neutrino. The cuts are therefore:

- The event must contain more than four tracks ($n_{ch} > 4$).
- Exactly one jet must have been reconstructed in the pseudorapidity region $|\eta_j| < 2$.
- No hit in the MIP plug with a significant charge deposition is found.
- The jet must consist of more than six particles ($n_{qj} > 6$).
- The distance of the primary vertex to the nominal interaction point has to be less than 2 cm.

The following cuts are applied to the 432 data events which remain after this preselection:

NQ1) The ratio between the jet energy E_{jet} and the total visible energy E_{vis} in the event has to be greater than 0.8 ($E_{jet}/E_{vis} > 0.8$). This cut is very effective in reducing all sources of Standard Model background like multihadronic and two-photon events.

NQ2) The difference between the jet transverse energy, $E_{\mathrm{T,jet}}$, and the missing transverse energy, $\not\!\!E_{\mathrm{T}}$, has to be less than 2 GeV ($|E_{\mathrm{T,jet}} - \not\!\!E_{\mathrm{T}}| < 2$ GeV) in order to ensure that the final state consists of a single jet balanced by missing transverse energy.

cuts		Pre-	$E_{\mathrm{jet}}/E_{\mathrm{vis}}$	$\lvert \mathrm{E_{T,jet}} - \not\!\!E_{\mathrm{T}} \rvert$
M_{LQ} (GeV/c^2)	state	selection	(NQ1)	(NQ2)
80	scalar	57.0%	45.4%	41.5%
120		62.3%	54.4%	48.3%
160		67.7%	65.6%	56.1%
80	vector	59.0%	43.6%	39.9%
120		59.2%	50.0%	43.7%
160		62.2%	60.1%	51.6%
$e^+e^- \to q\overline{q}$		178.2	2.9	0.0 ± 0.6
$e^+e^- \to \tau^+\tau^-$		4.6	2.1	0.3 ± 0.1
$e^+e^- \to 4$ fermions		71.0	10.5	6.3 ± 0.3
two-photon		172.4	4.6	2.4 ± 1.1
total BG		426.2	20.1	8.9 ± 1.2
data		432	24	7

Table 4: Selection efficiencies for three different leptoquark masses for scalar and vector leptoquarks. Also shown is the remaining number of data events and the expected number of background (BG) events after each cut of the neutrino plus hadronic jet selection. The Monte Carlo background is normalised to the data luminosity of 158.4 pb^{-1} at 189 GeV. The errors on the Monte Carlo background are statistical.

Table 4 shows the number of data and Monte Carlo events normalised to data luminosity after each cut beginning after the preselection. The signal efficiencies for three different scalar and vector leptoquark masses are also given. The efficiencies are similar for scalar and for vector states.

After all cuts, 7 events remain which is in good agreement with the Standard Model expectation of 8.9 ± 1.2 (stat) events. From the two-photon events only the CC DIS events give a sizeable contribution to the final background composition together with the hadronic four-fermion processes.

Fig. 5 shows some of the cut variables for data, Standard Model background and the leptoquark state $\tilde{\mathrm{S}}_{1/2}$ with a mass of 120 GeV/c^2 in arbitrary normalisation. The sum of the Standard Model Monte Carlo distributions describes the data sufficiently well. Fig. 6a) shows the selection efficiencies as determined with the scalar and vector leptoquarks generated with ERATO-LQ after all cuts as a

function of the generated leptoquark mass M_{LQ}. Fig. 6b) shows the distribution of the transverse mass $M_{\mathrm{T}} = 2\not{E}_{\mathrm{T}}$ after all cuts for data, Standard Model background, and for the state $\mathrm{S}_{1/2}$ using $\lambda = \sqrt{4\pi\alpha_{\mathrm{em}}}$ with $M_{\mathrm{LQ}} = 80$ GeV/c^2 and 120 GeV/c^2.

5 Results

The systematic errors on the expected signal rate are: (a) the luminosity measurement with less than 1 %, (b) the model dependence of the leptoquark fragmentation with 1 to 5 %, (c) the parameter dependence for the jet finding with 2 to 5 %, (d) the Monte Carlo statistics with 1 %.

A special version of PYTHIA has been used to study the difference between models where the hadronisation is simulated before and after the leptoquark decay into an electron and a quark [38]. The difference in the average charged multiplicity within the geometrical acceptance of the detector increases with leptoquark mass and is always less than one unit. The model dependence of the leptoquark fragmentation has therefore been estimated by varying the cut on the charged multiplicity by one unit in the Monte Carlo while keeping it fixed in the data since the charged multiplicity cut is expected to be very sensitive to the hadronisation model. In addition, the jet finding parameters have been varied: the value of the minimum transverse energy for a jet has been changed by ± 5 GeV and the jet radius R has been changed from 1 to 0.7. The effect from the variation of R is negligible.

The Monte Carlo model dependence has been studied by comparing the alternative background Monte Carlo sets defined in section 3. In the eq channel the alternative two-photon and four-fermion sample predict each an increase in the total number of background events of about 10%. This would lead to a higher limit on the leptoquark mass than the Monte Carlo sample used. For the νq-channel the four-fermion generators yield consistent results and the expected two-photon background decreases from 2.4 to 1.3 events, leading to a negligible change in the mass limits.

The systematic errors are added in quadrature and they are taken into account in the limit using the procedure of Highland and Cousins [39].

The limits have been calculated for three different values of the branching ratio $\beta = 1$, $\beta = 0.5$, and $\beta \to 0$, since for $\beta \equiv 0$ no production in eq collisions is possible. The limit calculations have been performed according to the procedure of [40] which takes into account the expected background, the mass resolution, the

candidates, and the efficiencies. The cross-section excluded at the 95% confidence level, σ_{95}, resulting from these calculations is shown in Fig. 7 for scalar and for vector leptoquarks. The resulting mass limits are given in Table 5 for $\lambda = \sqrt{4\pi\alpha_{\rm em}}$, where the electromagnetic coupling constant $\alpha_{\rm em}$ is taken at the mass of the leptoquark with $\alpha_{\rm em}(M_{\rm LQ}) \approx 1/128$. The upper limit at the 95 % CL of the coupling λ (λ') as a function of the mass $M_{\rm LQ}$ is given in Figs. 8 and 9.

charge	state	$\beta = 1$	$\beta = 0.5$	$\beta \to 0$
$\pm 1/3$	S_0, S_1, $\tilde{S}_{1/2}$,	163 GeV/c^2	158 GeV/c^2	175 GeV/c^2
$-5/3$	$S_{1/2}$	164 GeV/c^2	-	-
$-4/3$	$\tilde{S}_0$	149 GeV/c^2	-	-
$-4/3$	S_1	156 GeV/c^2	-	-
$-2/3$	$\tilde{S}_{1/2}$, $S_{1/2}$, $S_{1/2}$	121 GeV/c^2	-	141 GeV/c^2
$+2/3$	S_1	-	-	162 GeV/c^2

Table 5: Mass limits for scalar leptoquarks and squarks for $\lambda = \sqrt{4\pi\alpha_{\rm em}}$ and the different β values.

We have also derived the limit on $M_{\rm LQ}$ as a function of β for couplings of electromagnetic strength ($\lambda = \sqrt{4\pi\alpha_{\rm em}}$), i.e. the assumption is dropped that the branching ratio β can take only the values $0, 0.5$ and 1. In Fig. 12 the limit on β as a function of $M_{\rm LQ}$ is compared to the D0 results [14] which only exclude values up to $M_{\rm LQ} = 80$ GeV/c^2 for $\beta = 0$. Our analysis is more sensitive in the low β region, yielding a limit of $M_{\rm LQ} = 175$ GeV/c^2 for $\beta \to 0$. A similar region has recently been explored by H1 [10].

Exactly the same procedure as for scalar leptoquarks has been used to determine the mass limits and limits on the Yukawa coupling for vector leptoquarks. The systematic errors are also identical. The results for the mass limits are shown in Table 6. The upper limit at the 95 % CL of the coupling λ as a function of the mass $M_{\rm LQ}$ is given in Figs. 10-11.

5.1 Conclusions

We have searched for singly-produced leptoquarks in electron-photon interactions at an e^+e^- centre-of-mass energy of 189 GeV using the data collected with the OPAL detector at LEP. The data correspond to an integrated luminosity of about 160 pb^{-1}. Some scalar leptoquark states can also be identified with squarks in

charge	state	$\beta = 1$	$\beta = 0.5$	$\beta \to 0$
$-1/3$	$V_{1/2}$, $\tilde{V}_{1/2}$	176 GeV/c^2	-	182 GeV/c^2
$+1/3$	V_1	-	-	188 GeV/c^2
$-5/3$	$\tilde{V}_0$	177 GeV/c^2	-	-
$-5/3$	V_1	182 GeV/c^2	-	-
$-4/3$	$V_{1/2}$	152 GeV/c^2	-	-
$\pm 2/3$	V_0, V_1, $\tilde{V}_{1/2}$	151 GeV/c^2	149 GeV/c^2	163 GeV/c^2

Table 6: Mass limits for vector leptoquarks for $\lambda = \sqrt{4\pi\alpha_{\rm em}}$ and the different possible β values.

R-parity violating SUSY models. No evidence was found for the production of these particles. Therefore, 95% confidence limits were set on the mass as well as on the Yukawa coupling λ for scalar and vector leptoquarks and λ' for squarks as a function of the mass for different branching fractions β in eq final states.

Acknowledgements

We thank M. Doncheski, S. Godfrey and U. Katz for very useful discussions and C. Papadopoulos for his help in using ERATO-LQ.
We particularly wish to thank the SL Division for the efficient operation of the LEP accelerator at all energies and for their continuing close cooperation with our experimental group. We thank our colleagues from CEA, DAPNIA/SPP, CE-Saclay for their efforts over the years on the time-of-flight and trigger systems which we continue to use. In addition to the support staff at our own institutions we are pleased to acknowledge the
Department of Energy, USA,
National Science Foundation, USA,
Particle Physics and Astronomy Research Council, UK,
Natural Sciences and Engineering Research Council, Canada,
Israel Science Foundation, administered by the Israel Academy of Science and Humanities,
Minerva Gesellschaft,
Benoziyo Center for High Energy Physics,
Japanese Ministry of Education, Science and Culture (the Monbusho) and a grant under the Monbusho International Science Research Program,
Japanese Society for the Promotion of Science (JSPS),
German Israeli Bi-national Science Foundation (GIF),

Bundesministerium für Bildung und Forschung, Germany,
National Research Council of Canada,
Research Corporation, USA,
Hungarian Foundation for Scientific Research, OTKA T-029328, T023793 and OTKA F-023259.

References

[1] W. Buchmüller, R. Rückl and D. Wyler, Phys. Lett. B191 (1987) 442.

[2] J. Kalinowski, R. Rückl, H. Spiesberger and P.M. Zerwas, Z. Phys. C74 (1997) 595.

[3] H.P. Nilles, Phys. Rep. 110 (1984) 1;
H.E. Haber and G.L. Kane, Phys. Rep. 117 (1985) 75.

[4] M.A. Doncheski and S. Godfrey, Phys. Lett. B393 (1997) 355;
M.A. Doncheski and S. Godfrey, Mod. Phys. L. A12 (1997) 1719 and private communications.

[5] T.M. Aliev, E. Iltan and N.K. Pak, Phys. Rev. D54 (1996) 4263.

[6] G. Bélanger, D. London and H. Nadeau, Phys. Rev. D49 (1994) 3140.

[7] J. Blümlein and E. Boos, Nucl. Phys. Proc. Suppl. B37 (1994) 181.

[8] J.L. Hewett, S. Pakvasa, Phys. Lett. B227 (1987) 178.

[9] DELPHI Collab., P.P. Allport et al, Phys. Lett. B446 (1999) 62.

[10] H1 Collab., C. Adloff et al, Eur. Phys. J. C11 (1999) 447.

[11] ALEPH Collab., R. Barate et al, Eur. Phys. J. C12 (2000) 183;
OPAL Collab., G. Abbiendi et al, Eur. Phys. J. C6 (1999) 1;
L3 Collab, M. Acciari et al, Phys. Lett. B433 (1998) 163.

[12] DELPHI Collab., P. Abreu et al., Phys. Lett. B316 (1993) 620;
DELPHI Collab., P. Abreu et al., Phys. Lett. B275 (1992) 222;
ALEPH Collab., D. Decamp et al., Phys. Rept. 216 (1992) 253;
OPAL Collab., G. Alexander et al., Phys. Lett. B263 (1991) 123;
L3 Collab, B. Adeva et al., Phys. Lett. B261 (1991) 169.

[13] OPAL Collab., G. Abbiendi et al, Eur. Phys. J. C13 (2000) 15.

[14] D0 Collab., B. Abbott et al., Phys. Rev. Lett. 83 (1999) 2896;
D0 Collab., B. Abbott et al., Phys. Rev. Lett. 80 (1998) 2051.

[15] CDF Collab., F. Abe et al., Phys. Rev. Lett. 82 (1999) 3206;
CDF Collab., F. Abe et al., Phys. Rev. Lett. 81 (1998) 4806;
CDF Collab., F. Abe et al., Phys. Rev. Lett. 79 (1997) 4327;
CDF Collab., F. Abe et al., Phys. Rev. Lett. 75 (1995) 1012

[16] C. Grosso-Pilcher et al., *Combined Limits on First Generation Leptoquarks from the CDF and D0 Experiments*, FERMILAB-PUB-98-312-E, hep-ex/9810015.

[17] D0 Collab., B. Abbott et al., Phys. Rev. Lett. 83 (1999) 4476;
D0 Collab., F. Abe et al., Phys. Rev. Lett. 83 (1999) 2133;
CDF Collab., B. Abbott et al., Phys. Rev. Lett. 83 (1999) 4937;
CDF Collab., F. Abe et al., Phys. Rev. D56 (1997) 1357.

[18] ALEPH Collab., R. Barate et al., *Search for R-Parity Violating Decays of Supersymmetric Particles in e^+e^- Collisions at Center-of-Mass Energies from 189 GeV to 202 GeV*, CERN-EP-2000-132;
DELPHI Collab., P. Abreu et al., Eur. Phys. J. C13 (2000) 591;
OPAL Collab., G. Abbiendi et al., Eur. Phys. J. C12 (2000) 1;
L3 Collab., M. Acciarri et al., Phys. Lett. B459 (1999) 354.

[19] OPAL Collab., K. Ahmet et al., Nucl. Instr. and Meth. A305 (1991) 275.

[20] S. Anderson et al., Nucl. Instr. and Meth. A403 (1998) 326.

[21] OPAL Collab., K. Ackerstaff et al., Eur. Phys. J. C12 (2000) 551.

[22] B.E. Anderson et al., IEEE Transactions on Nuclear Science 41 (1994) 845.

[23] OPAL Collab., K. Ackerstaff et al., Phys. Lett. B391 (1997) 221.

[24] P. Aurenche and G. A. Schuler (conveners), $\gamma\gamma$ *Physics*, in "Physics at LEP2", CERN 96-01, eds. G. Altarelli, T. Sjöstrand and F. Zwirner, Vol. 1 (1996) 291.

[25] C. Papadopoulos, Comp. Phys. Comm. 118 (1999) 118;
C. Papadopoulos, Comp. Phys. Comm. 101 (1997) 183.

[26] T. Sjöstrand, Comp. Phys. Comm. 82 (1994) 74.

[27] M. Glück, E. Reya and A. Vogt, Phys. Rev. D46 (1992) 1973;
M. Glück, E. Reya and A. Vogt, Phys. Rev. D45 (1992) 3986.

[28] G.A. Schuler and T. Sjöstrand, Z. Phys. C68 (1995) 607.

[29] S. Jadach, B.F.L. Ward and Z. Wąs, Comp. Phys. Comm. 79 (1994) 503.

[30] S. Jadach, W. Płaczek, B.F.L. Ward, in 'Physics at LEP2', eds. G. Altarelli, T. Sjöstrand and F. Zwirner, CERN 96-01, vol.2 (1996).

[31] G. Marchesini, B.R. Webber, G. Abbiendi, I.G. Knowles, M.H. Seymour and L. Stanco, Comp. Phys. Comm. 67 (1992) 465.

[32] R. Engel and J. Ranft, Phys. Rev. D54 (1996) 4244;
R. Engel, Z. Phys. C66 (1995) 203.

[33] J.A.M. Vermaseren, Nucl. Phys. B229 (1983) 347.

[34] A. Buijs, W. G. J. Langeveld, M. H. Lehto and D.J. Miller, Comp. Phys. Comm. 79 (1994) 523.

[35] J. Fujimoto et al., in "Physics at LEP2", eds. G. Altarelli, T. Sjöstrand and F. Zwirner, CERN 96-01, Vol. 2 (1996).

[36] S. Jadach, W. Placzek, M. Skrzypek, B.F. Ward and Z. Wąs, Comput. Phys. Commun. 119 (1999) 272.

[37] OPAL Collab., K. Ackerstaff et al., Z. Phys. C73 (1997) 433.

[38] C. Friberg, E. Norrbin, T. Sjöstrand, Phys. Lett. B403 (1997) 329 and private communications.

[39] R.D. Cousins and V.L. Highland, Nucl. Inst. and Meth. A320 (1992) 331.

[40] P. Bock, *Determination of exclusion limits for particle production using different decays channels with different efficiencies, mass resolutions and backgrounds*, Heidelberg University, HD-PY-96/05 (1996).

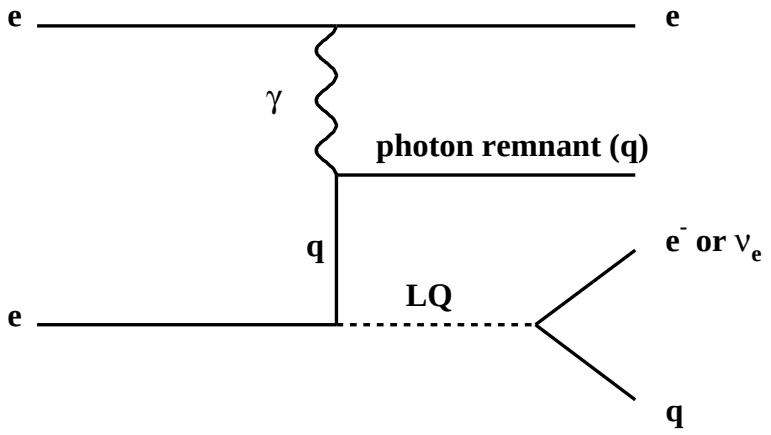

Figure 1: Diagram of the s-channel production of a leptoquark (LQ) in electron-photon scattering. The photon is radiated by one of the LEP beams, fluctuates into a hadronic object and one of the quarks interacts with an electron from the other beam.

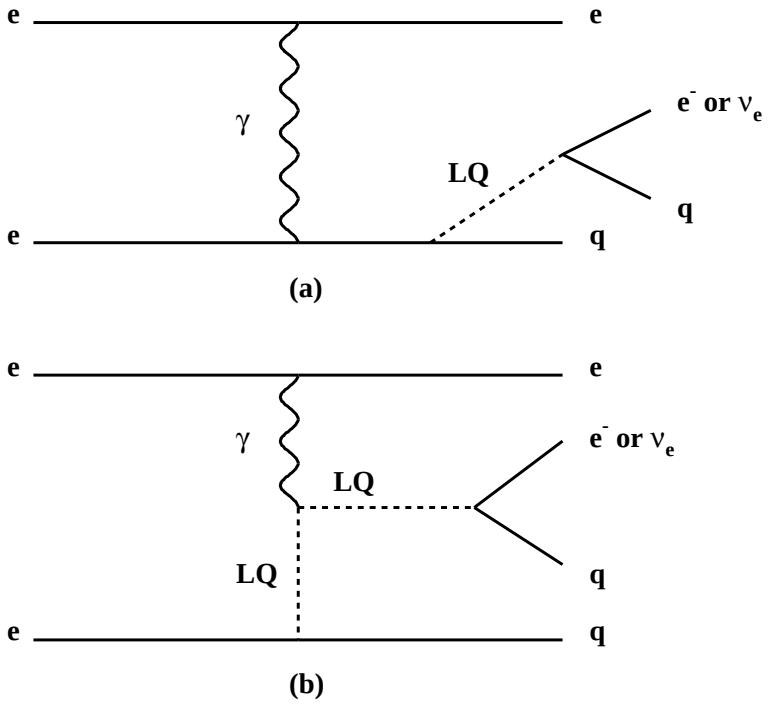

Figure 2: Alternative single leptoquark production mechanisms, where the photon interacts pointlike: (**a**) "direct" interaction with the beam electron, (**b**) photon is absorbed by the leptoquark "emitted" by the other beam electron.

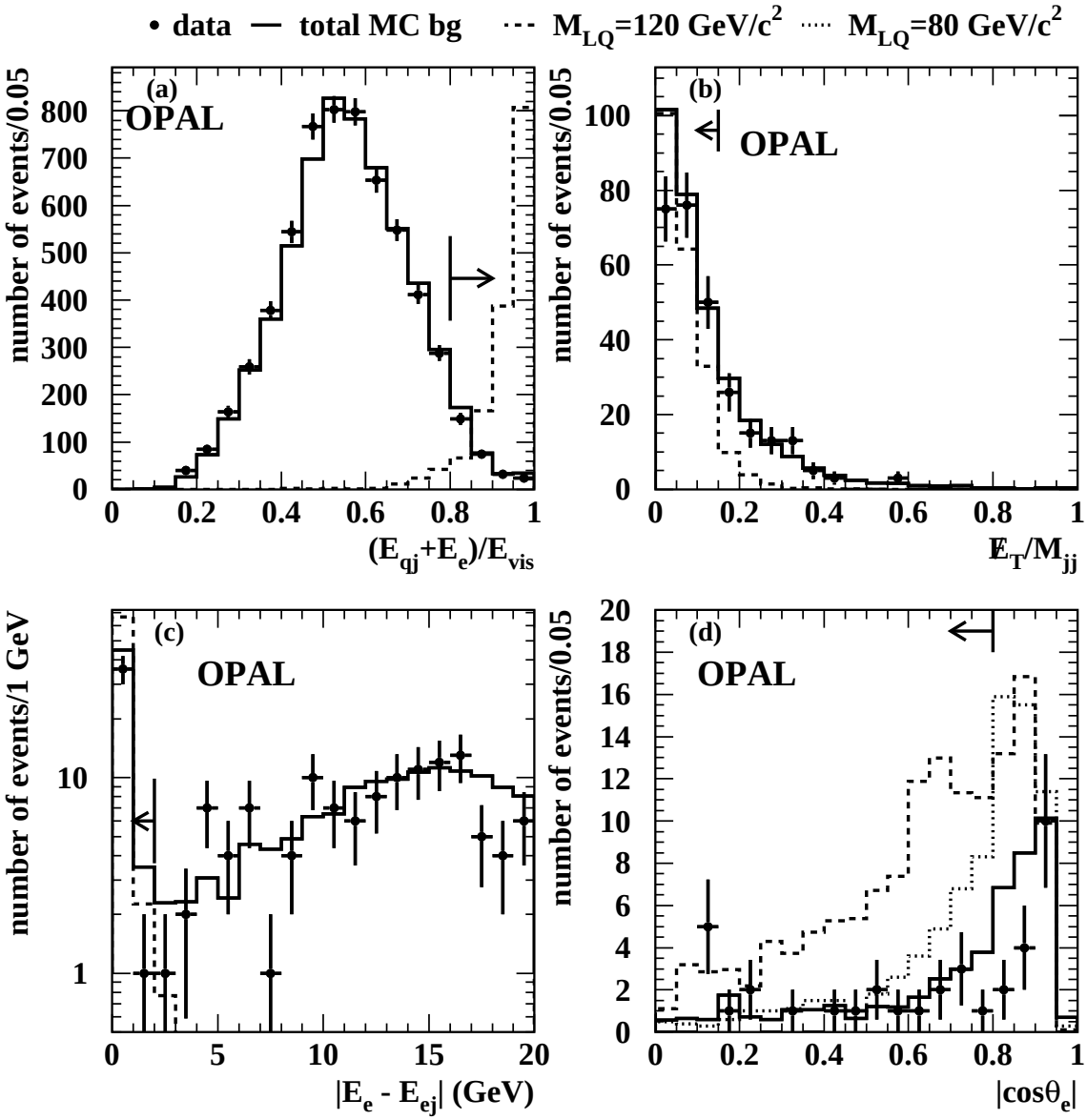

Figure 3: Electron-quark decay channel: (**a**) distribution of the ratio $(E_{\rm qj} + E_{\rm e})/E_{\rm vis}$ after the preselection; (**b**) distribution of the ratio $\not\!\!E_{\rm T}\,/M_{\rm jj}$ after applying the additional cut EQ1; (**c**) distribution of the difference $|E_{\rm e} - E_{\rm ej}|$ after applying the additional cut EQ2; (**d**) distribution of the electron scattering angle $|\cos\theta_{\rm e}|$ after applying cuts EQ1 through EQ3 to the preselected data. The points with error bars are the data, the full line represents the total Standard Model background normalised to data luminosity and the dashed (dotted) histogram shows the distribution for the vector leptoquark state $\tilde{\rm V}_0$ with a mass of 120 GeV/c^2 (80 GeV/c^2). The normalisation of the leptoquark signals is arbitrary.

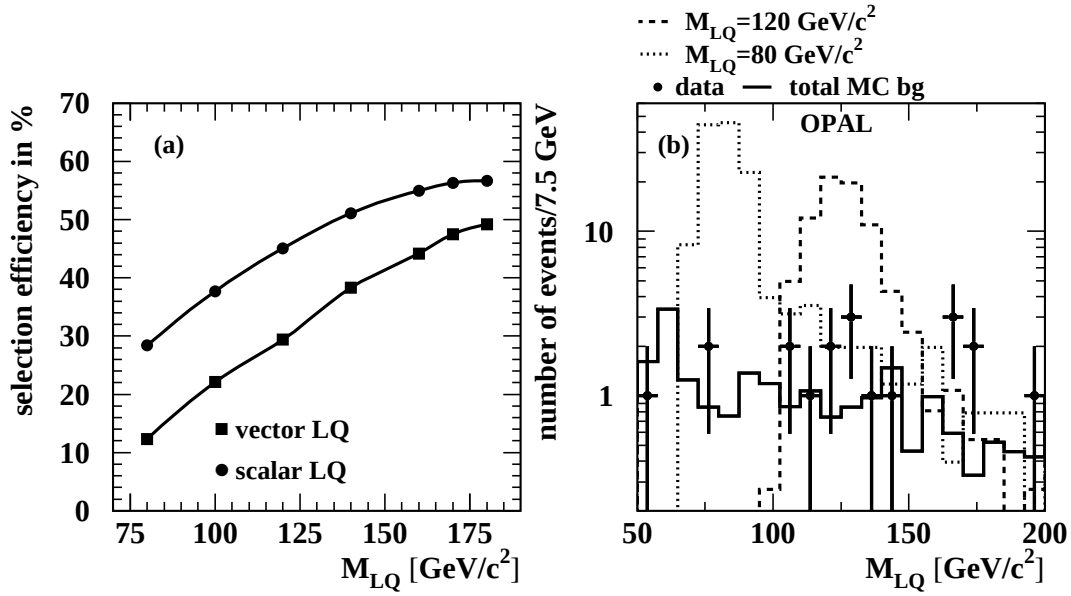

Figure 4: (**a**) Selection efficiency in the eq channel after all cuts for scalar (dots) and vector (squares) leptoquarks; (**b**) Invariant mass $M_{\rm jj}$ of the two jets (= leptoquark mass) after all cuts for data (points with error bars), Standard Model background (full line) and two different vector leptoquark masses (dotted line for 80 GeV/c^2 and dashed line for 120 GeV/c^2). The state $\tilde{\rm V}_0$ was chosen to normalise the signal, using $\lambda = \sqrt{4\pi\alpha_{\rm em}}$.

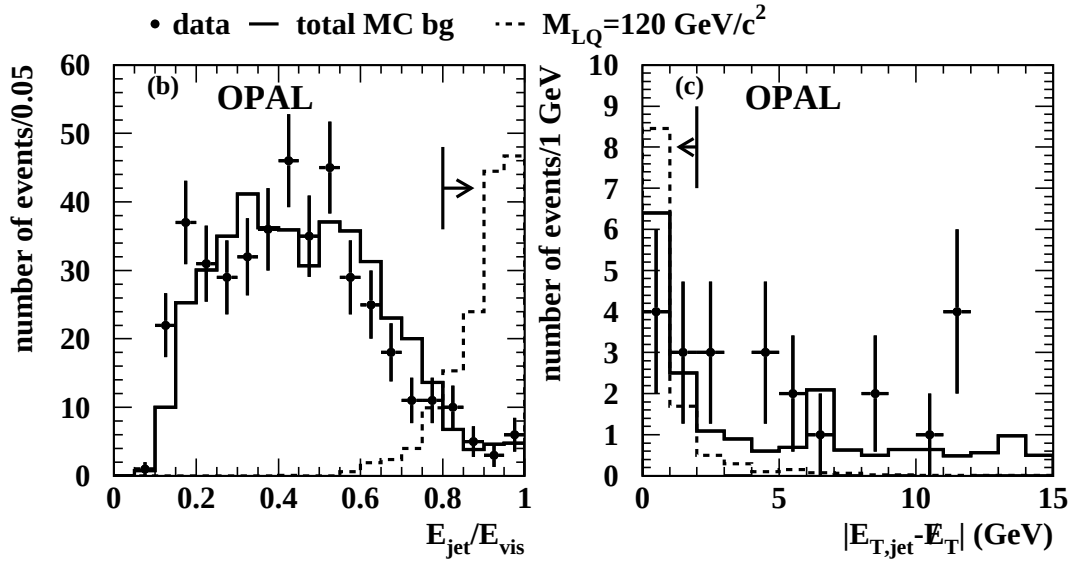

Figure 5: Neutrino-quark decay channel: (**a**) distribution of the ratio $E_{\rm jet}/E_{\rm vis}$ after the preselection; (**b**) distribution of the variable $|E_{\rm jet} - \not{E}_{\rm T}|$ after the cut NQ1 ($(E_{\rm jet}/E_{\rm vis} > 0.8)$. The points with error bars are the data, the full line represents the total Standard Model background normalised to data luminosity and the dashed histogram shows the distribution for the scalar state $S_{1/2}$ with a mass of 120 GeV/c^2. The normalisation of the leptoquark signals is arbitrary.

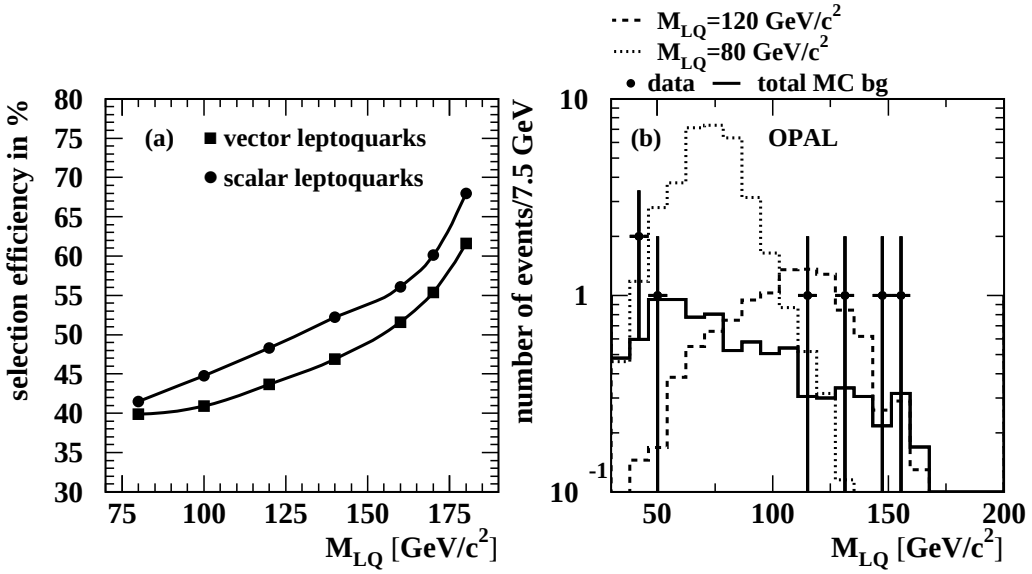

Figure 6: (**a**) Selection efficiency in the νq channel after all cuts for scalar (dots) and vector (squares) leptoquarks; (**b**) transverse mass $M_{\mathrm{T}} = 2\not{E}_{\mathrm{T}}$ after all cuts for data (points with error bars), Standard Model background (full line) and two different scalar leptoquark masses (dotted line for 80 GeV/c^2 and dashed line for 120 GeV/c^2). The state $\mathrm{S}_{1/2}$ (charge -2/3) was chosen to normalise the signal, using $\lambda = \sqrt{4\pi\alpha_{\mathrm{em}}}$.

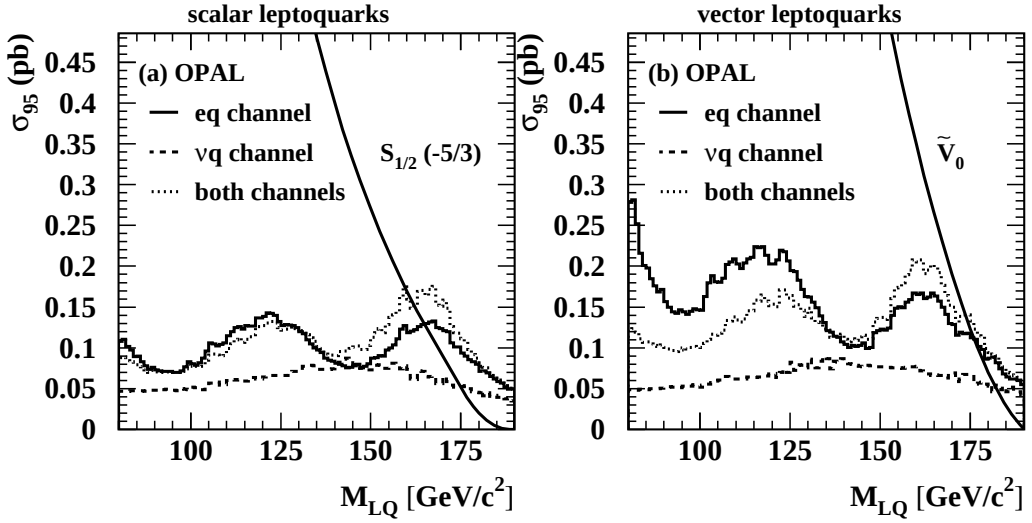

Figure 7: Cross-section excluded at the 95% confidence level, σ_{95}, using the number of candidates in the data for each channel separately, corresponding to β=1 for the electron-quark channel (full line) and β=0 for the neutrino-quark channel (dashed line), as well as for equal branching ratio into both channels (β=0.5, dotted line). The expected SM background, the mass resolution, the candidates, and the efficiencies are taken into account in the calculation. The cross-section for the production of the states a) $\mathrm{S}_{1/2}$ (charge $-5/3$) and b) $\tilde{\mathrm{V}}_0$ are also shown.

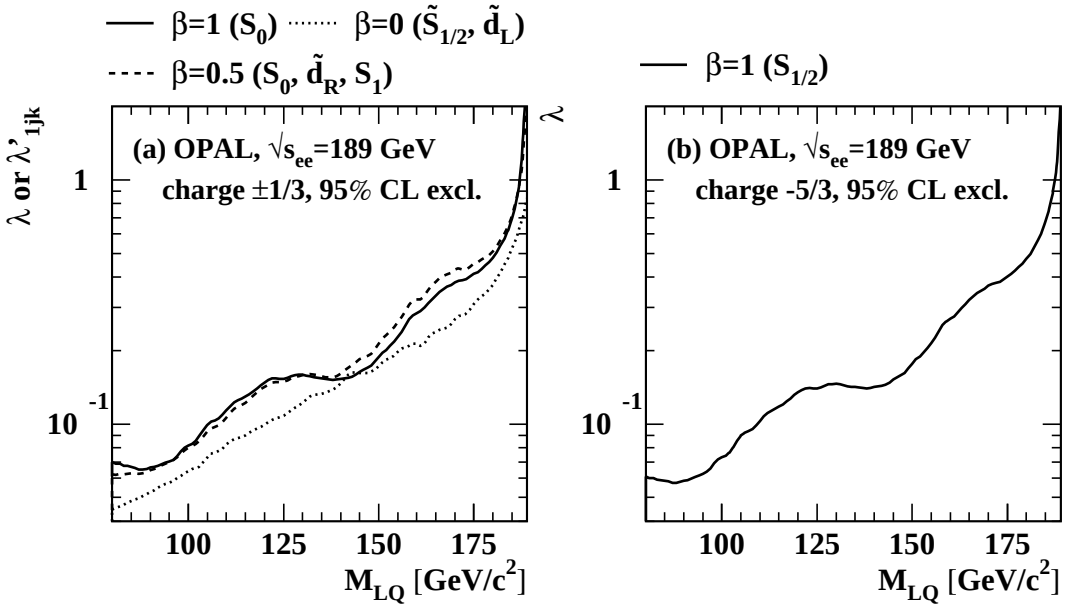

Figure 8: Limits on the coupling constants λ (λ'_{1jk}) for scalar leptoquark states (squarks) with (**a**) charge $\pm\frac{1}{3}$: S_0 with $\beta = 1$ (full line), S_0, $\tilde{d}_R$, S_1 with $\beta = 0.5$ (dashed line) as well as $\tilde{S}_{1/2}$ and $\bar{\tilde{d}}_L$ with $\beta = 0$ (**b**) charge $-\frac{5}{3}$: $S_{1/2}$ with $\beta = 1$.

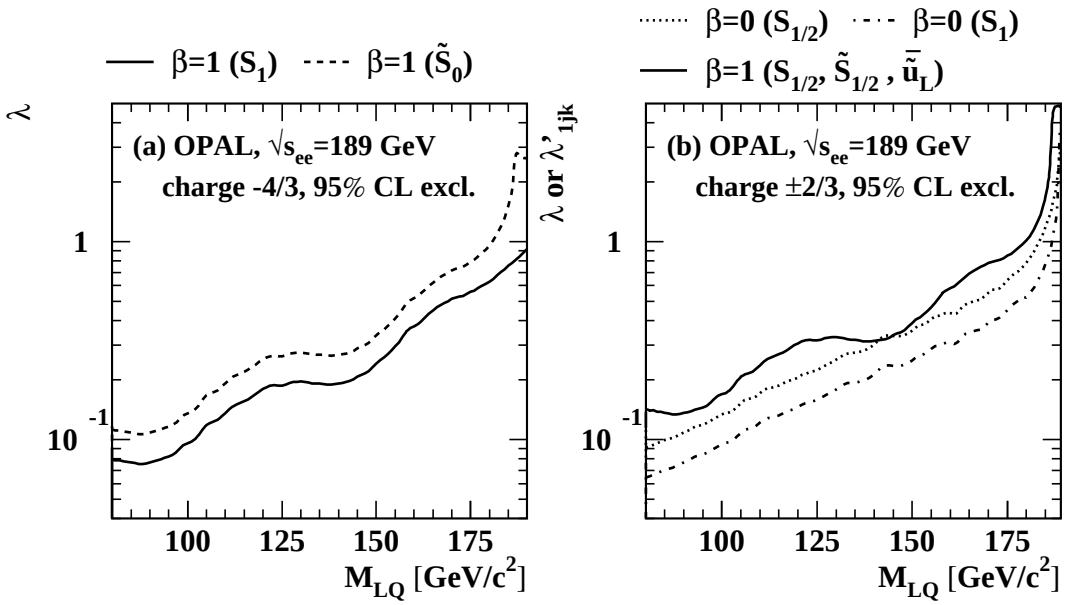

Figure 9: Limits on the coupling constant λ (λ'_{1jk}) for scalar leptoquark states (squarks) with (**a**) charge $-\frac{4}{3}$: S_1 with $\beta = 1$ (full line), $\tilde{S}_0$, with $\beta = 1$ (dashed line) (**b**) charge $\pm\frac{2}{3}$: $\tilde{S}_{1/2}$, $\bar{\tilde{u}}_L$, $S_{1/2}$ with $\beta = 1$ (full line), $S_{1/2}$ with $\beta = 0$ (dotted line) and S_1 with $\beta = 0$ (dashed-dotted line).

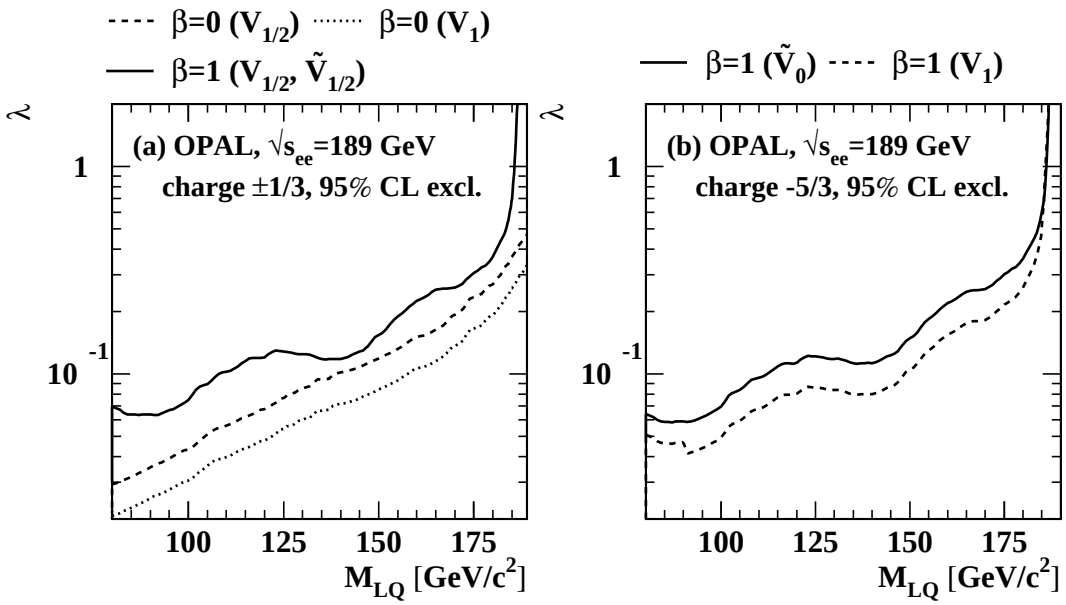

Figure 10: Limits on the coupling constant λ for vector leptoquark states with (**a**) charge $\pm\frac{1}{3}$: $V_{1/2}$,$\tilde{V}_{1/2}$ with $\beta = 1$ (full line) and $V_{1/2}$, V_1 with $\beta = 0$ (**b**) charge $-\frac{5}{3}$: $\tilde{V}_0$ with $\beta = 1$ (full line) and V_1 with $\beta = 1$ (dashed line).

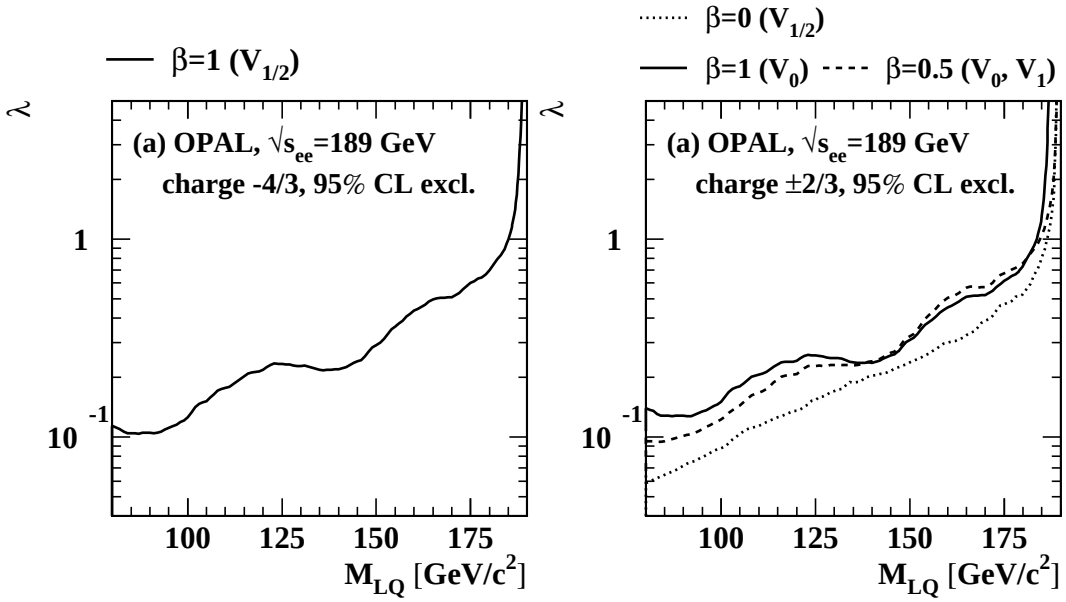

Figure 11: Limits on the coupling constant λ for vector leptoquark states with (**a**) charge $-\frac{4}{3}$: $V_{1/2}$ with $\beta = 1$ (full line) (**b**) charge $\pm\frac{2}{3}$: V_0 with $\beta = 1$ (full line), V_0, V_1 with $\beta = 0.5$ (dashed line) and $V_{1/2}$ with $\beta = 0$ (dotted line).

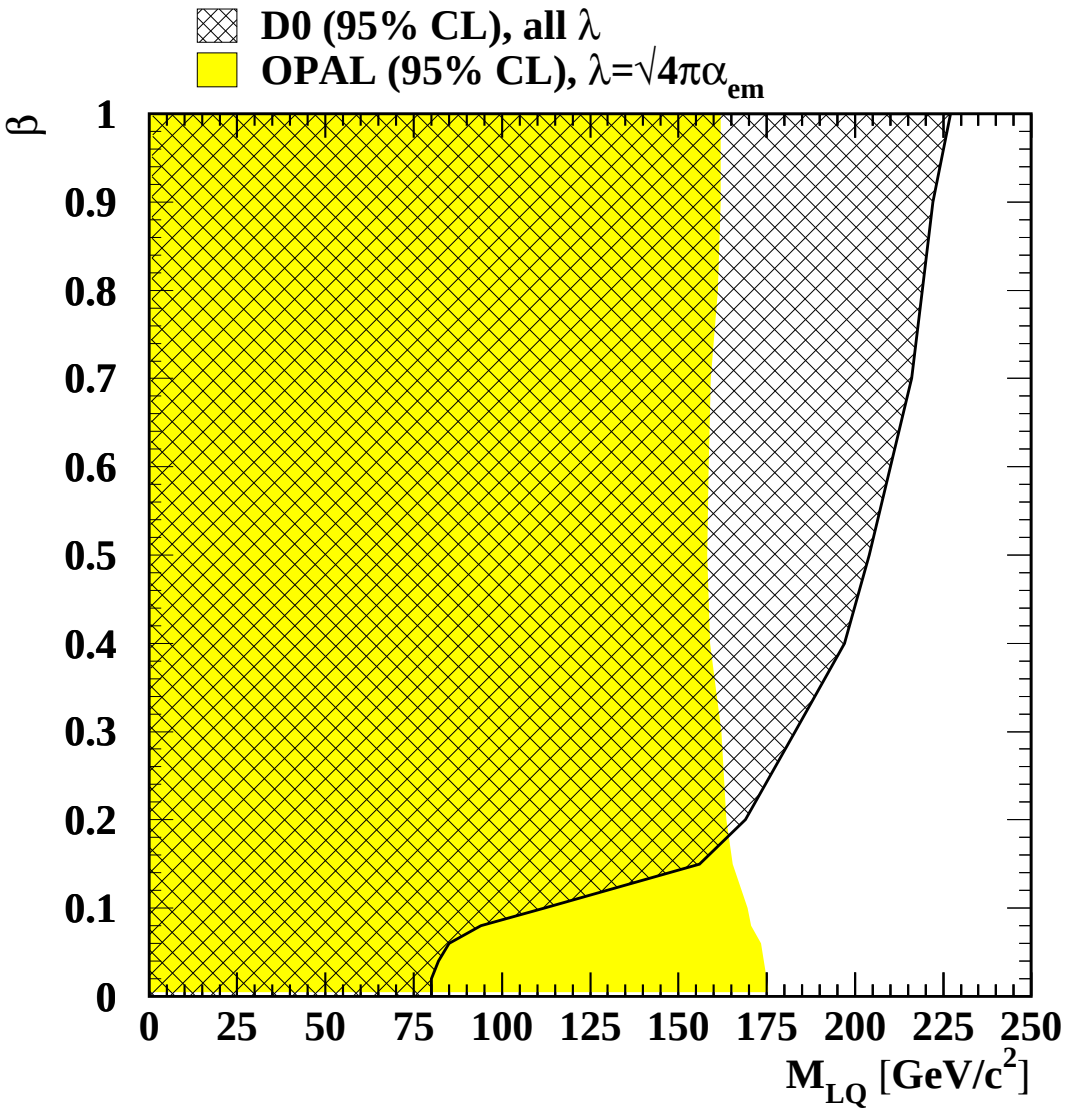

Figure 12: Limit on $M_{\rm LQ}$ as a function of β for couplings of electromagnetic strength ($\lambda = \sqrt{4\pi\alpha_{\rm em}}$) for the charge $\pm 1/3$ scalar states. The limit on β is compared to the D0 results [14]. For $\beta \equiv 0$ no production in eq collisions is possible.